Structural basis for the broad-spectrum inhibition of metallo-beta-lactamases by thiols

Structural basis for the broad-spectrum inhibition of metallo-β-lactamases by thiols†

Benoît M. R. Liénard,[a] Gianpiero Garau,‡[b] Louise Horsfall,[c] Andreas I. Karsisiotis,§[d] Christian Damblon,§[d] Patricia Lassaux,[c] Cyril Papamicael,¶[a] Gordon C. K. Roberts,[d] Moreno Galleni,[c] Otto Dideberg,[b] Jean-Marie Frère[c] and Christopher J. Schofield*[a]

Received 25th February 2008, Accepted 25th March 2008
First published as an Advance Article on the web 7th May 2008
DOI: 10.1039/b802311e

The development of broad-spectrum metallo-β-lactamase (MBL) inhibitors is challenging due to structural diversity and differences in metal utilisation by these enzymes. Analysis of structural data, followed by non-denturing mass spectrometric analyses, identified thiols proposed to inhibit representative MBLs from all three sub-classes: B1, B2 and B3. Solution analyses led to the identification of broad spectrum inhibitors, including potent inhibitors of the CphA MBL (*Aeromonas hydrophila*). Structural studies revealed that, as observed for other B1 and B3 MBLs, inhibition of the L1 MBL thiols involves metal chelation. Evidence is reported that this is not the case for inhibition of the CphA enzyme by some thiols; the crystal structure of the CphA–Zn–inhibitor complex reveals a binding mode in which the thiol does not interact with the zinc. The structural data enabled the design and the production of further more potent inhibitors. Overall the results suggest that the development of reasonably broad-spectrum MBL inhibitors should be possible.

Introduction

β-Lactamases (BLs) are classified into those employing a nucleophilic serinyl residue (classes A, C and D) and those binding one or two zinc ions (metallo-β-lactamases, MBLs, class B) at their active site. Medicinal attention has primarily focused on the serine BLs, and inhibitors of these enzymes are widely used. However, MBLs hydrolyze most β-lactam antibiotics and are an increasing clinical problem (for a review see ref. 1). MBLs can be divided into three subclasses on the basis of their substrate selectivity. Sub-classes B1 and B3 display a broad substrate selectivity whereas sub-class B2 most efficiently hydrolyze carbapenems.[2,3] B1 MBLs, including BcII (*Bacillus cereus*) and IMP-1 (*Pseudomonas aeruginosa*), can employ either one or two active site Zn(II) ions, whereas B3 MBLs, *e.g.* FEZ-1 (*Legionella gormanii*) and L1 (*Stenotrophomonas maltophilia*), are only active with two Zn(II) ions. The B2 MBL CphA (*Aeromonas hydrophilia*) is active as a mono-zinc protein but is non-competitively inhibited by the presence of a second Zn(II).[4] Crystal and solution structures of representatives from the three subclasses reveal significant structural differences in the active site pocket[5–7] and in a loop involved in substrate binding.[8,9]

The active site metal-binding chemistry and structural variations make the development of broad-spectrum MBL inhibitors challenging. At present, there are no reports of individual MBL inhibitors with sub-micromolar K_i values against all three MBL sub-classes; however, such a property will be highly desirable, if not a prerequisite, for a clinically useful compound. Thiols are the most studied MBL inhibitors, with various derivatives having been described (*e.g.* thiomandelic acid,[10] D-captopril,[11] 6-(mercaptomethyl)penicillinates,[12] homocysteinyl-containing peptides[13] and derivatives of mercaptobenzoic acid).[14] (±)-Thiomandelic acid (**1**) and D-captopril (**2**) are reported to be potent inhibitors of sub-classes B1 and B3. However, **1** and **2** fail to potently inhibit members of the B2 sub-class (K_i = 144 μM for **1**, and 72 μM for **2**), and thus are probably not useful broad-spectrum inhibitors.

Here we report how the application of MS-based screening coupled to structural analyses led to the identification of broad-spectrum inhibitors of clinically relevant metallo-β-lactamases.

Initial screening and assays

With the aim of identifying molecules capable of inhibiting MBLs from all three sub-classes, we analysed X-ray structures for representative MBLs from the three sub-classes: BcII (B1), IMP-1 (B1), CphA (B2), L1 (B3) and FEZ-1 (B3) (Fig. 1).

Based on the structural analyses, selected thiols were then synthesised (Scheme 1) and screened for binding to representative MBLs (BcII, CphA and FEZ-1) using electrospray ionisation-MS

[a]*Chemistry Research Laboratory and OCISB, University of Oxford, 12 Mansfield Road, Oxford, OX1 3TA, UK. E-mail: Christopher.schofield@chem.ox.ac.uk; Fax: +44 (0) 1865 275 674; Tel: +44 (0) 1865 275 625*
[b]*Institut de Biologie Structurale Jean-Pierre Ebel (CNRS/CEA/UJF), 41 Rue J. Horowitz, Grenoble, 38100, France*
[c]*Centre d'Ingéniérie des Protéines, Université de Liège, Allée de 6 Aout B6, Sart-Tilman, Liège, Belgium*
[d]*Henry Wellcome Laboratories of Structural Biology, Biochemistry Department, University of Leicester, Rm 1/02, Henry Wellcome Building, Lancaster Road, Leicester, LE1 9HN, UK*

† Electronic supplementary information (ESI) available: X-Ray crystallographic data; additional NMR data. See DOI: 10.1039/b802311e

‡ Current address: Biocrystallography Unit, San Raffaele Scientific Institute, DIBIT, via Olgettina 58, 20132 Milano, Italy.
§ Current address: Centre de Biophysique Moléculaire, UPR 4301 CNRS, rue Carles Sadron, 45071 Orléans Cedex 2, France.
¶ Current address: Laboratoire de Chimie Fine et Hétérocyclique UMR 6014 IRCOF, CNRS, Université et INSA de Rouen, BP 08, 76131, Mont-Saint-Aignan Cedex, France.

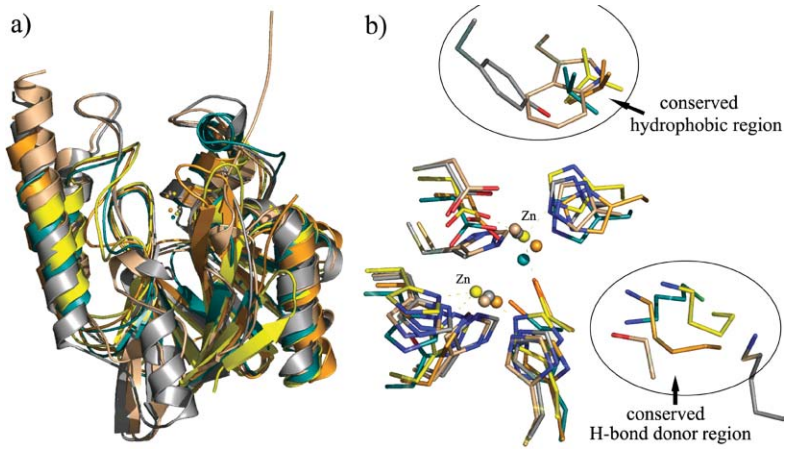

Fig. 1 Superimposition of views derived from the crystal structures of BcII (sub-class B1, orange, PDB code 1BVT),[15] IMP-1 (sub-class B1, yellow, PDB code 1DDK),[8] CphA (sub-class B2, blue, PDB code 18XI),[5] L1 (sub-class B3, pink, PDB code 1SML)[16] and FEZ-1 (sub-class B3, grey, PDB code 1K07).[17] (a) Overall folds and (b) close-up of selected residues at the active sites (nitrogen in blue, oxygen in red and sulfur in orange). The figure highlights the overall structural similarities between these MBLs, including between the dizinc-binding enzymes (BcII, IMP-1, L1 and FEZ-1) and the monozinc-binding MBLs (*e.g.* CphA, in blue). The numbering scheme is that for the BcII enzyme. Figure made using LSQMAN and PyMOL.

under non-denaturing ionisation conditions (Fig. 2). Although there are limitations to the use of MS for screening for enzyme inhibitors,[18–21] ESI-MS has been productively used to analyse the binding of inhibitors to MBLs including in dynamic thiol exchange methodology.[14]

Compound **3** was prepared in three steps as reported (16% overall yield)[22] (Scheme 1a). α-Mercaptoketone **4** was prepared from commercially available α-bromoketone (65% overall yield; all yields unoptimised) (Scheme 1b). α-Bromoketone **16** was alkylated using potassium thioacetate to give **17**, then hydrolysed to give **4**. **5a,b** and **8a–c** were prepared, using an alternative to the reported methods,[22,23] in three steps from the corresponding amino acids (overall yields: 12 to 48%) (Scheme 1c). Thus 3-bromopropionyl chloride was treated with the methyl ester of suitable amino acid hydrochlorides to give bromides **18–22**. Substitution using potassium thioacetate gave acetylthiolates **23–27**; subsequent hydrolysis of the protecting groups led to the formation of mercaptocarboxylates **5a,b** and **8a–c** in moderate

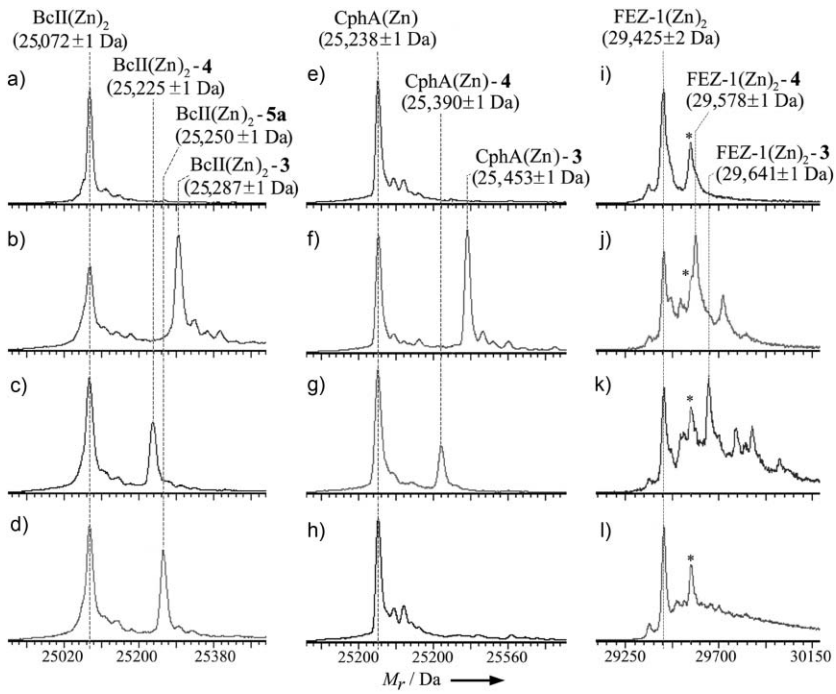

Fig. 2 Deconvoluted ESI-MS spectra under non-denaturing conditions showing a) BcII–Zn_2, b) BcII–Zn_2 + **3** (1 eq.), c) BcII–Zn_2 + **4** (1 eq.), d) BcII–Zn_2 + **5a** (1 eq.), e) CphA–Zn, f) CphA–Zn + **3** (1 eq.), g) CphA–Zn + **4** (1 eq.), h) CphA–Zn + **5a** (1 eq.), i) FEZ-1–Zn_2, j) FEZ-1–Zn_2 + **3** (1 eq.), k) FEZ-1–Zn_2 + **4** (1 eq.) and l) FEZ-1–Zn_2 + **5a** (1 eq.). * FEZ-1–Zn_2 + methionine (N-terminal ± methionine residue was confirmed by tryptic digestion followed by MALDI-MS analyses).

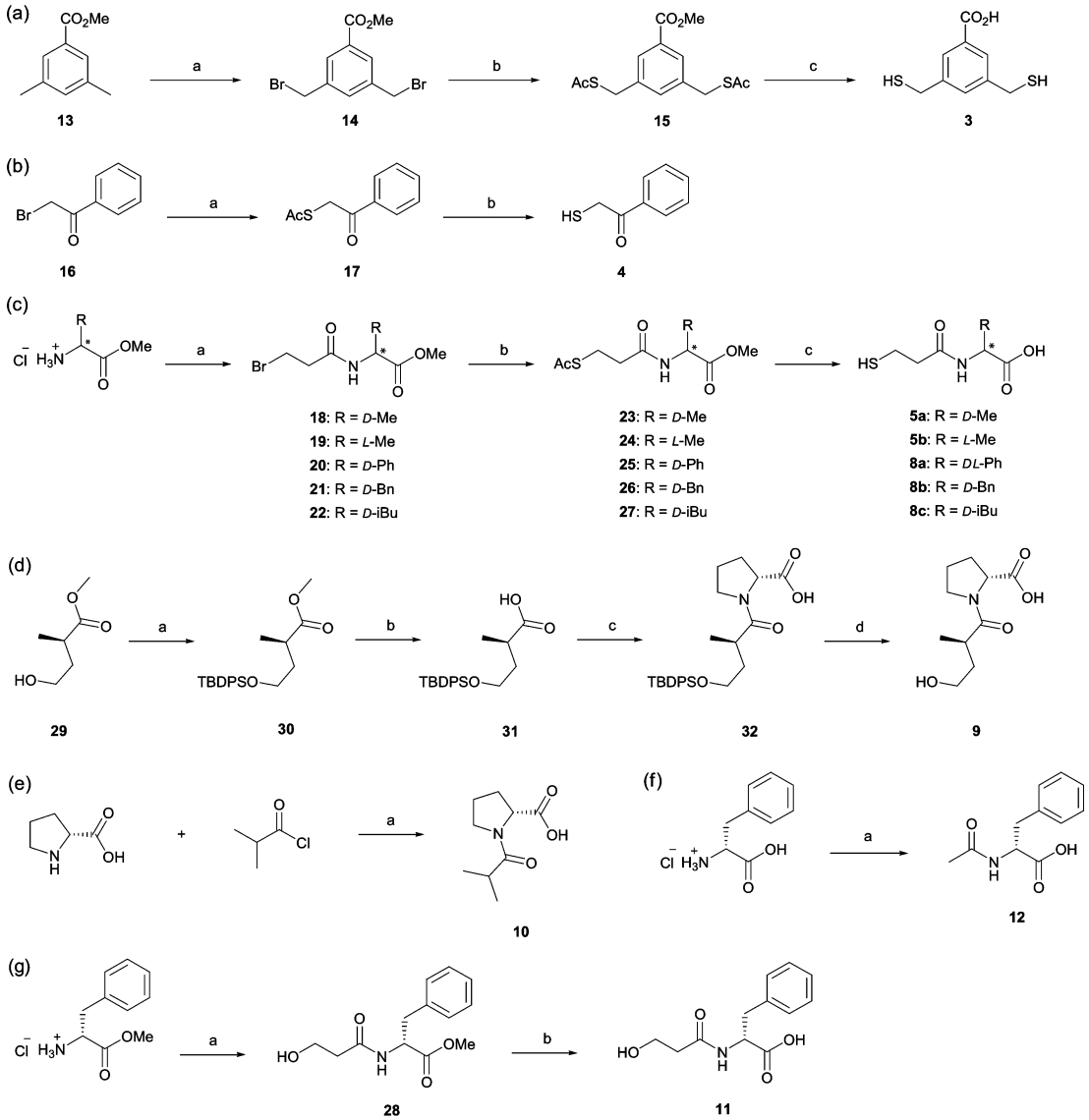

Scheme 1 *Reagents and conditions*: **(a)** a) NBS, dibenzoyl peroxide, CCl_4, reflux, 1.5 h, 28%; b) AcSK, EtOAc, rt, 14 h, 69%; c) NaOH (1 N), 70 °C, 3 h, 82%. **(b)** a) AcSK, CH_2Cl_2, rt, 14 h, 94%; b) NaOH (1 N), rt, 6 h, 69%. **(c)** a) 3-bromopropionyl chloride, $NaHCO_3$ (5% aq.), CH_2Cl_2, rt, 1–3 h, 22–99%; b) AcSK, EtOAc, rt, 12 h, 54–99%; c) NaOH (1 N), 70 °C, 1.5 h, 88–97%. **(d)** a) TBDPSCl, imidazole, DMF, rt, 12 h, 65%; b) LiOH, THF–MeOH, 0 °C → rt, 20 h, 89%; c) (i) $(COCl)_2$, benzene, 0 °C, 3 h; (ii) D-proline, Et_3N, rt, 18 h, 76%; d) HF·pyridine, THF, rt, 12 h, 50%. **(e)** a) Et_3N, dioxane–H_2O, −10 °C → rt, 18 h, 73%. **(f)** a) NaOH (4 N), AcCl, 0 °C, 1 h, 41%. **(g)** a) β-propiolactone, AcONa, EtOH, 0 °C→rt, 15 h, 21%; b) NaOH (1 N), rt, 15 h, 53%.

yields. D-Phenylglycine derivative **8a** was obtained as a racemic mixture in the last deprotection step. Compound **9** was prepared in two steps from D-phenylalanine methyl ester hydrochloride (22% overall yield) (Scheme 1d). Protection of commercially available alcohol **29** using *tert*-butyldiphenylsilyl chloride (TBDPSCl) and imidazole to give **30**, followed by methyl ester hydrolysis (LiOH) gave **31** in good yield. Carboxylic acid **31** was converted into the corresponding acyl chloride (oxalyl chloride), which was then reacted with D-proline to give carboxylic acid **32** in good overall yield. Deprotection of the silyl group using fluoridric acid in pyridine afforded the desired hydroxycarboxylic acid in reasonable yield. **10** was prepared in one step from D-proline (Scheme 1e). **11** was prepared in two steps from D-phenylalanine methyl ester hydrochloride (11% overall yield) (Scheme 1g). **12** was prepared in one step from D-phenylalanine in 41% yield under Schotten–Baumann conditions (Scheme 1f).[24]

With the exceptions of **5a** and **5b**, which were not observed to bind significantly to CphA and FEZ-1 by ESI-MS under the applied experimental conditions, two of the tested compounds (**3** and **4**, Fig. 3) showed a significant ability to form enzyme–metal–ligand complexes with all the tested MBLs; CphA–Zn–**5a** or **5b** and FEZ-1–Zn_2–**5a** or **5b** complexes were observed when an excess of **5a,b** was used (data not shown). Thiols **5a,b** are less functionalised derivatives of the reported MBL inhibitors **6** and **7** (see below).[8,25] Thiols **3** and **4** formed significant CphA–Zn–ligand complexes (Fig. 2d,e), but did not induce the binding of a second zinc ion in the active site of CphA as reported for **1**.[14] These results implied that the distance between the thiol and the

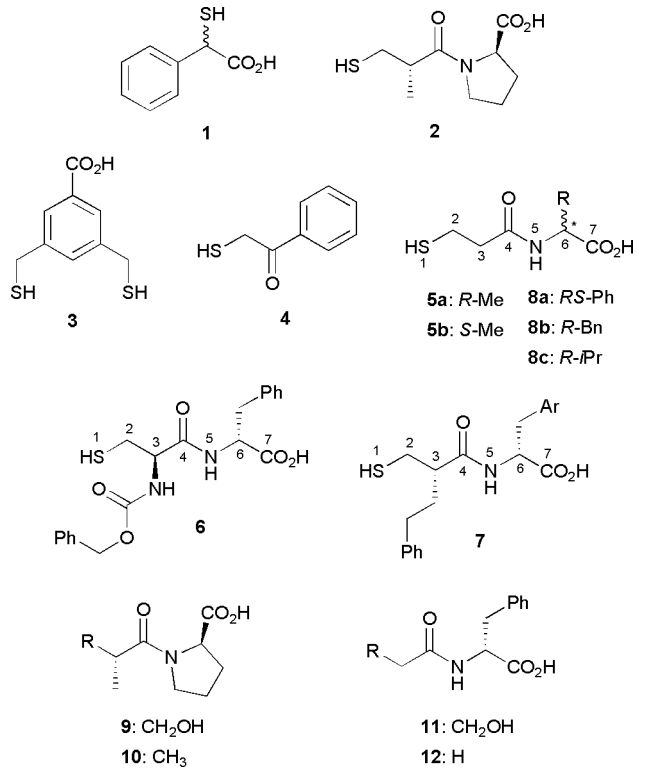

Fig. 3 Structures of the thiols and their derivatives under investigation in this study.

carboxylate groups of inhibitors not only influences the potency of MBL inhibition by mercaptocarboxylate, as proposed,[10] but can also influence the mechanism of inhibition *via* modification of the MBL–metal–ligand stoichiometry, *i.e.* **1** binds as a CphA–Zn_2–ligand complex but **3** and **4** bind as CphA–Zn–ligand complexes (at least by MS analyses).

Compounds **3–5** were then screened for inhibition against MBLs from all three sub-classes (Table 1). Strikingly, **3** and **4** were found to inhibit all the tested MBLs. **3** is the first reported broad spectrum MBL inhibitor with K_i values <1 μM for all MBLs. **3** ($K_i = 90$ nM) and **4** ($K_i = 50$ nM) were the most potent reported inhibitors for the monozinc CphA MBL (Table 1).

The results also imply that mercaptocarboxylate compounds that bind as CphA–Zn complexes rather than CphA–Zn_2 complexes are more potent CphA inhibitors; thus, thiol **4**, which appears to bind as a monozinc complex to CphA (by ESI-MS), is *ca.* 3000 times more potent than **1**, which binds to the CphA MBL preferentially as a dizinc complex.[14] Compounds **5a** and **5b** were found to significantly inhibit sub-classes B1 and B3 MBLs but not the sub-class B2 CphA MBL, in partial agreement with the ESI-MS studies. For comparison, **6** displays a K_i value of 0.3 μM *vs.* BcII[25] and **7** K_i values of 0.1–0.5 μM *vs.* IMP-1, BcII and L1 (Fig. 3).[8]

Modelling and NMR studies

To investigate the broad-spectrum nature of the inhibition of **4**, docking studies were carried out with representatives of each sub-class (IMP-1, CphA and L1). Initially, to test the utility of the modelling technique, **7** was docked into IMP-1–Zn–**7**[8] (with **7** extracted) using different zinc coordination geometries (data not shown). A close correlation between the structure of the IMP-1–Zn–**7** complex in the reported X-ray structure[8] and the highest scoring docked conformation was obtained using a tetrahedral geometry for both active site zinc cations. A trigonal bipyramidal geometry was used for the monozinc CphA based on the previously reported crystallographic data for the complexed CphA structure.[5] In all cases, the choice of the metal coordination type of the enzyme as well as the parametrisation of the ligand (*i.e.* ionisation state of the thiol/carboxylate groups and the tautomeric form of the amide bond) were found to be important for good correlation between the binding mode observed in the crystal structures and the modelling data. Generally, for dizinc MBLs, the lowest rms deviations between the MBL–Zn_2–ligand crystal structures and the highest scoring modelled structures were obtained when using deprotonated SH/CO_2H groups and the amide tautomer form of the inhibitor. Conversely, the use of deprotonated SH/CO_2H and the imidic acid tautomer form achieved the most consistent results (and the highest docking scores) for the monozinc CphA. These observations highlight the influence of the preparation of molecules for docking studies with metalloenzymes.

Compound **4** was predicted to interact with the dizinc MBLs (IMP-1 and L1) *via* a metal bridging chelation involving its thiolate and a hydrogen-bond between its carbonyl group and the conserved MBL hydrogen-bond donor region (Fig. 1, Fig. 4a,c). The proposed bridging metal chelation of **4** is precedented by various crystallographic and solution studies on dizinc MBLs.[7,8,11,17] In contrast, the modelling studies led to the prediction that both the thiolate and carbonyl groups of **4** chelate the monozinc ion CphA (Fig. 4b), indicating a potential for the same inhibitor to adopt different (predominant) binding modes to different MBLs. Docking of **3** resulted in a more complex analysis due to several possible predicted structures for the MBL–**3** complexes (data not shown). However, the results suggested that the key

Table 1 Competitive inhibition constants K_i (μM)

	B1		B2	B3	
Compound	IMP-1	BcII	CphA	L1	FEZ-1
3	0.36 ± 0.01	0.97 ± 0.2	0.09 ± 0.004	0.21 ± 0.01	0.3[a]
4	0.67 ± 0.09	2.7 ± 0.2	0.05 ± 0.02	0.24 ± 0.01	1[a]
5a	68 ± 30	5.6 ± 0.3	—[b]	6.5 ± 2	240 ± 50
5b	7.5 ± 5	37 ± 1	—[b]	37 ± 0.7	42 ± 1

[a] IC_{50}. [b] Not determined.

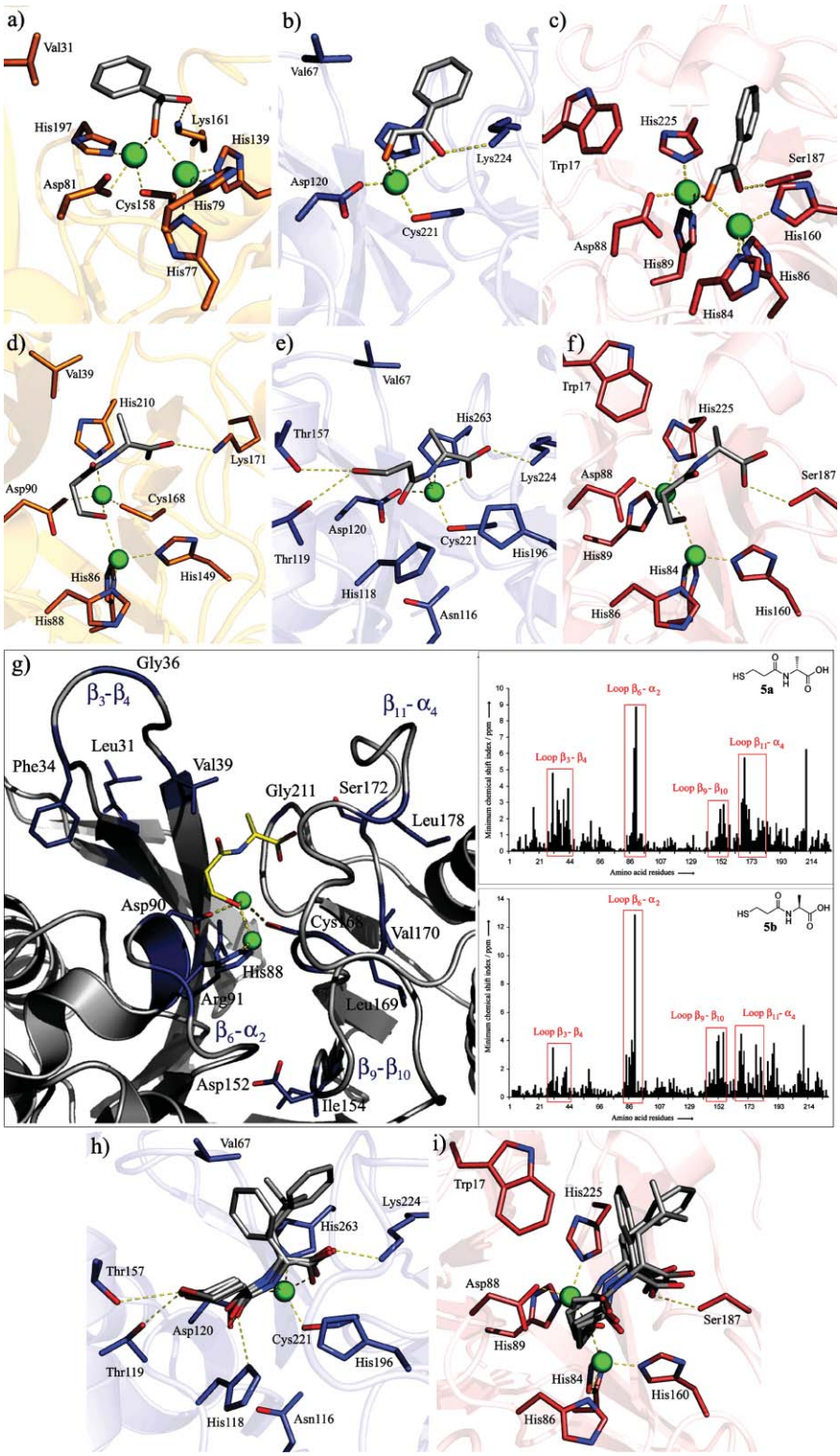

Fig. 4 Results of docking studies (using GOLD) of **4** (carbon atoms in grey) complexed with a) IMP-1 (PDB ID: 1DDK),[8] b) CphA (PDB ID: 1X8G)[5] and c) L1 (PDB ID: 1SML)[16] MBLs, highlighting the potential for different binding modes. Results of docking studies (using GOLD) for **5a** (carbon atom in grey) complexed with d) BcII (PDB ID: 1BVT),[15] e) CphA (PDB ID: 1X8G)[5] and f) L1 (PDB ID: 1SML)[16] MBLs. Results of NMR analyses of the BcII–Zn_2 MBL with **5a** showing g) the most significantly affected BcII residues (dark blue) by the presence of **5a** mapped onto the predicted structure of BcII–Zn_2–**5a** complex (Fig. 4d) (left panel). This was determined using minimum chemical shift index calculations[26] on BcII–Zn_2–**5a** as well as on BcII–Zn_2–**5b** for comparison (right panels). Superimposition of the results of the docking studies of (h) **5a**, **8a**, **8b** and **8c** (carbon atoms are in grey) in complex with CphA (PDB ID: 1X8G)[5] and (i) **5a** and **8a**,**c** in complex with L1 (PDB ID: 1SML).[16] Only the D-isomer of **8c** was tested. The zinc ions are represented as green spheres. Figure made using PyMOL.

enzyme–inhibitor interactions involve the carboxylate group of **3** with the conserved hydrogen-bond region (Fig. 1) and its thiolate group with the two zinc ions. **5a** was predicted to bind similarly to the dizinc MBLs with similar interactions predicted for **3** and **4**, *i.e.* the C-7 carboxylate of **5a** interacting with the MBL hydrogen-bond donor region and the thiolate with the zinc ions (Fig. 4d and Fig. 5f). In contrast, when **5a** was docked into the monozinc MBL CphA the results suggested that **5a** may chelate to the zinc cation *via* its C-7 carboxylate and imidic acid nitrogen (Fig. 4e). In this mode the C-4 carbonyl of **5a** can interact with the side chains of Asp120 and His118 and the thiolate group is positioned to make hydrogen bonds with the hydroxyl side chains of Thr119 and Thr157, *i.e.* not to the zinc ions. Although not precedented by any structural work on thiol MBL inhibitors, this binding mode is

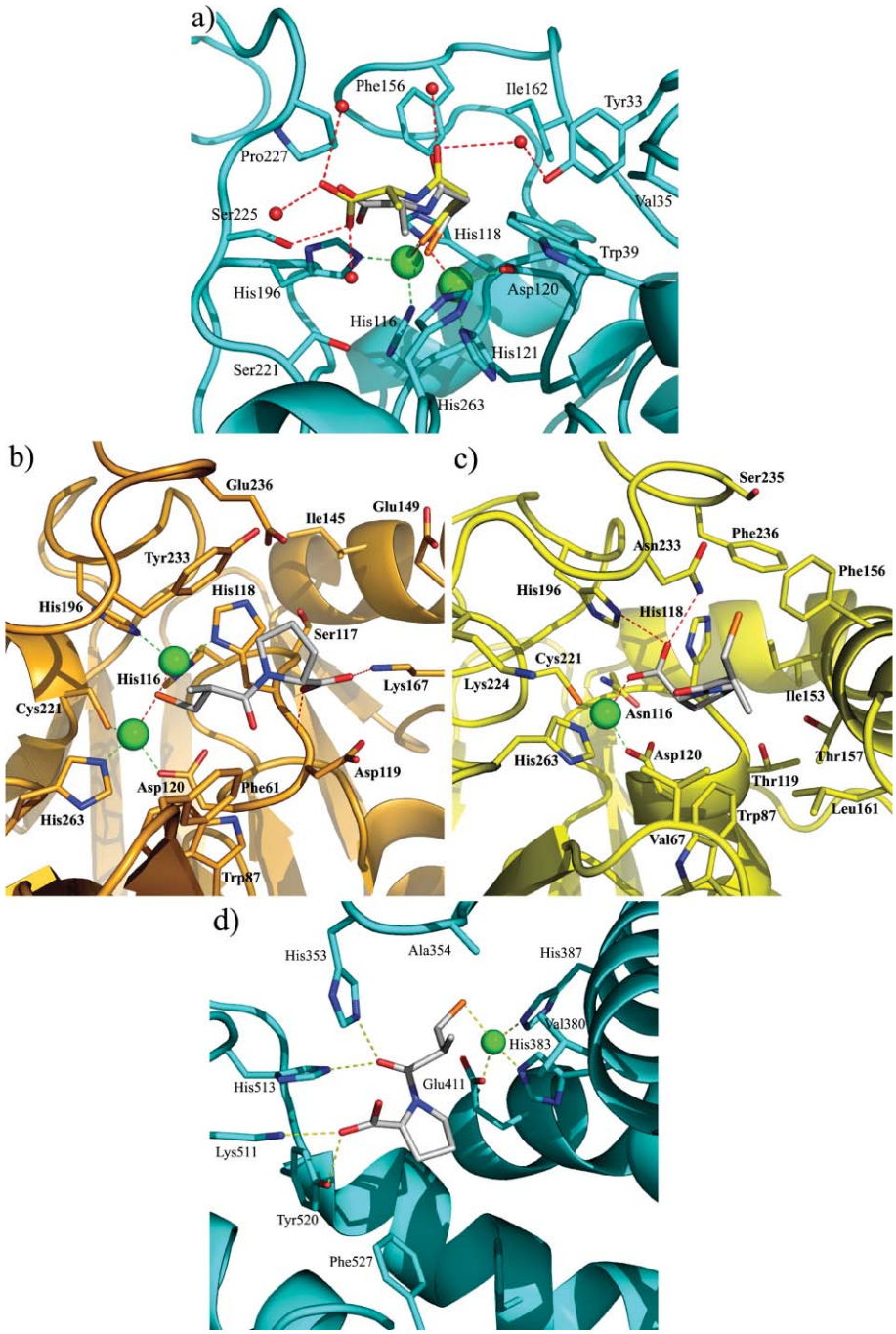

Fig. 5 a) Active site view from a crystal structure of L1–Zn_2 in complex with **5a** (carbon atoms in yellow, PDB ID: 2QDT). Only water molecules (red spheres) forming H-bonds with **5a** are shown; the figure highlights the good correlation between the binding mode of **5a** to L1–Zn_2 from the crystallographic data (carbon atoms coloured in yellow) and the binding mode for **5a** predicted from modelling studies (carbon atoms coloured in grey). View from the active sites of b) BlaB (PDB ID: 1M2X),[27] in complex with **2** (carbon atoms in grey) c) CphA (PDB ID: 2QDS) in complex with **2** (carbon atoms in grey) and d) Angiotensin Converting Enzyme (ACE) (PDB ID: 1UZF)[28] in complex with **2** (carbon atoms in grey). The zinc ions are in green.

consistent with the reported mode of zinc chelation in the complex between hydrolysed biapenem and CphA.[5]

These modelling studies suggested that the inhibition of CphA may be enhanced by hydrophobic interactions with residues such as Val67, possibly explaining the lack of significant inhibition of **5a,b** (at 100 μM) *vs.* CphA. Significantly they also suggest that mercaptocarboxylates do not always inhibit monozinc MBLs *via* a thiol–zinc interaction.

To obtain structural information on the binding of **5a,b** to the sub-class B1 MBL and to test the modelling studies, NMR studies of BcII–Zn_2 with **5a** and **5b** were then carried out. The imidazole resonances of the metal binding histidine residues (His86, His88, His149 and His210)[6] are useful probes of the effects of inhibitors. In the absence of inhibitors, relatively sharp resonances were observed for His86 and His88 and a broad resonance for His210, but the signal of His149 was too broad to be detected. Titration of BcII–Zn_2 with **5a** resulted in a progressive decrease in the intensity of the imidazole NH signals of the free enzyme and a progressive increase in a new set of signals assigned to the enzyme–inhibitor complex (see ESI†). The intensity of the new peaks increased with the concentration of the inhibitor but their chemical shift was not affected. This behaviour is typical of a slow exchange between complexed and free enzyme, as observed for other compounds of the same class.[10]

Through the use of ^{1}H–^{15}N HSQC experiments optimized to detect long range ^{1}H–(C)–^{15}N couplings in the imidazole ring the resonance assignments for the histidine Hδ2 and Hε1 protons (C–H), along with the Hδ1 and Hε2 (N–H) protons and the corresponding nitrogens, can be obtained.[6] Analysis of the imidazole resonances for His88 and His210, which belong to different zinc binding sites, suggests that **5a** binds predominantly in a single conformation, whereas **5b** binds in two, or perhaps three, conformations (see ESI†).

The inhibitor titrations for **5a** and **5b** reveal that **5a** binds more tightly to BcII than does **5b**, an observation consistent with their respective K_i values. The chemical shift changes, in the form of minimum chemical shift indices,[26] indicate that the binding of both compounds affects residues in the same loops near the active site (Fig. 4g, right panels). Both **5a** and **5b** affect backbone amide resonances corresponding to the loops β6–α2 (84–88), β9–β10 (144–154), β11–α4 (168–188); in general, the minimum chemical shift difference index is somewhat greater for **5b**, particularly for residues 83–91, 142–149 and 186–192. In terms of the chemical shift index, Asp90 and Arg91 are some of the BcII residues most affected by binding of **5a,b**, as previously observed for mercaptocarboxylate inhibitors.[10]

Compound **5a** appears to make significantly more interactions with the "mobile" β3–β4 BCII loop, compared to **5b** (Fig. 4g, left panel). Potent MBL inhibition has already been linked to the ability of an inhibitor to induce the β3–β4 loop closure.[8,9] **5a** but not **5b** was observed to make a significant interaction with Val39 from the β3–β4 loop in solution, consistent with the modelling studies (Fig. 4d) and with our hypothesis for the design of **5a** derivatives, *i.e.* the increase of the interactions with this conserved hydrophobic region.

Compound **5a** apparently makes significant interactions with metal-coordinating histidines at both zinc coordination sites, and therefore its binding likely involves the previously observed bridging interaction between its thiolate and the two zincs. **5a** also interacts significantly with the β3–β4 loop and the MBL conserved hydrophobic region, probably *via* its Cα methyl group.

Derivatives of 5a

We then sought to identify more potent inhibitors. Superimposition of the predicted L1–Zn_2–**5a** complex with the IMP-1, BcII, CphA and FEZ-1 crystal structures revealed that (i) the methyl group of **5a** could be positioned to make an interaction with the hydrophobic region conserved in all MBL active sites (Fig. 1) and (ii) derivatisation of **5a** at the C-2 and/or C-3 positions (such as in compounds **6** and **7**) would likely lead to structural clashes with the sub-class B2 CphA active site. These analyses prompted preparation of derivatives of **5a** with bulkier hydrophobic groups at C-6; it was proposed that increasing the hydrophobicity at the C-6 position as well as restricting substitution at the C-2/C-3 positions would increase the potency *vs.* the B1 and B3 sub-classes and activity *vs.* the CphA MBL. Starting from the appropriate amino acids, **8a–c** (Fig. 3) were synthesised in three steps from DL-phenylglycine, D-phenylalanine and D-valine, respectively (Scheme 1c).

Compounds **8a–c** inhibited all the MBLs tested with K_i values as low as 19 nM (Table 2). CphA was also inhibited by **8a–c** with K_i values in the low micromolar range, *i.e.* these compounds are up to 20 times more potent at inhibiting CphA than **2**. ESI-MS analyses (see ESI†) conducted with **8a–c** and CphA also indicated the preferential formation of CphA–Zn–ligand complexes (and not CphA–Zn_2–ligand such as observed with **1**), supporting the importance of the monozinc-binding inhibition mode for potent inhibition of the CphA MBL by this thiol series (**8a–c** were up to 40 times more potent than **1** *vs.* CphA).

To investigate how **8a–c** bind to MBLs, with both one and two active site zinc ions, further modelling analyses were then carried out. On this basis, all derivatives **8a–c** were predicted (i) to interact with the zinc ions through chelation of the thiolate function (except for CphA), (ii) to have a near-superimposable backbone with the lead molecule **5a**, (iii) to interact with the conserved hydrophobic region of the MBL active sites (Fig. 1) and (iv) to have a similar binding mode *vs* the dizinc enzymes BcII, IMP-1, L1 and FEZ-1 (Fig. 4h). The docking of **8a–c** with monozinc CphA resulted in high docking scores and suggested a near-identical binding mode to that of **5a** to CphA, *i.e.* without a thiol–metal interaction, with an apparent increase in the hydrophobic interactions with the side chain of Val67 (Fig. 4i).

Crystallographic analyses

To investigate the inhibition mechanism of **5a,b** and derivatives **8a–c** as well as to further test the modelling studies, we then co-crystallised **5a** in complex with the sub-class B3 L1 MBL (Fig. 5a).

Table 2 Competitive inhibition constants K_i (μM)[a]

Compound	IMP-1	BcII	CphA	L1
8a	0.019 ± 0.002	7.7 ± 0.7	5.7 ± 2.0	1.8 ± 0.4
8b	0.088 ± 0.010	0.85 ± 0.08	15.0 ± 5.0	0.96 ± 0.08
8c	0.063 ± 0.009	0.32 ± 0.01	3.6 ± 0.3	0.082 ± 0.002

[a] For experimental conditions see Kinetic analyses section below.

Analysis of the interactions between **5a** and the L1 enzyme active site showed that the inhibitor thiolate bridges the two Zn(II) ions (S^-–Zn1 = 2.3 Å; S^-–Zn2 = 2.4 Å). The **5a** inhibitor carboxylate group is positioned to form a hydrogen-bond with the Ser225 side chain (2.6 Å). Hydrophobic contacts apparently occur between the inhibitor methyl group in C-6 and His263 (4.1 Å) and Trp39 (4.2 Å), and between C4–C7 and the side chains of His118 (3.7 Å), Phe156 (4.1 Å) and Pro227 (3.5 Å). Furthermore, the crystal structure of L1–Zn_2–**5a** is in agreement with and supports the docking studies (Fig. 5a).

There is no reported X-ray diffraction study on the mode of binding of thiols to mono-zinc MBLs. To gain insight into the proposed binding mode of thiols such as **5a,b** and **8a–c** with the monozinc CphA MBL, where the modelling analyses suggested that the thiol does not chelate to the zinc, we attempted crystallisation of CphA–ligand complexes. We were able to obtain crystals of CphA–Zn in complex with **2**, which diffracted to 1.7 Å resolution (Fig. 1c). As revealed from the crystal structure of BlaB–Zn_2–**2** complex (*Chryseobacterium meningosepticum*),[27] **2** acts as an inhibitor of sub-class B1 di-zinc MBLs with bridging of its thiolate group between the two active site metal ions (Fig. 5b), as previously established for other thiolate inhibitors.[7,8] **2** has also the ability to interact with monozinc enzymes *via* its thiolate group as reported with an Angiotensin Converting Enzyme (ACE)–Zn–**2** crystal structure in which the thiolate function occupies the single tetrahedral coordination site left by the zinc-binding triad residues (Fig. 5d).[28]

In contrast to the crystal structures of the L1–Zn_2–**5a** complex (Fig. 5a) and the BlaB–Zn_2–**2** complex (Fig. 5b) and in agreement with the modelling predictions (Fig. 4h), the binding of **2** in the crystalline state was not by chelation to the zinc ion. Instead the main metal interactions between **2** and the monozinc CphA occur through the inhibitor carboxylate group, which coordinates a tetrahedrally cooordinated zinc ion (O2–Zn 2.1 Å) (Fig. 5c). The carboxylate O1 of **2** is positioned to hydrogen-bond with the side chains of His196 (3.1 Å) and Asn233 (2.7 Å). These residues approach the carboxylate group upon inhibitor binding *via* "closure" of the mobile loop, observed previously for the CphA enzyme.[5] The sulfhydryl group of **2** likely forms hydrophobic contacts with Phe156 (3.6 Å) and the side chain of Arg233 (3.8 Å) as well as with Trp87 (3.9 Å), Leu161 (3.9 Å) and Val67 (4.0 Å). It is notable that, in contrast to the data for the Zn(II) complex reported here, evidence from EXAFS and PAC indicates that in the Cd(II)-substituted form of CphA, **2** appears to bind the zinc ion preferentially *via* its thiolate group.[11] Inhibitors such as Enalapril or Lisinopril (non-thiol analogues of **2**) are reported to interact with the active site zinc ion of ACE *via* their carboxylate group, which occupies a similar position relative to the metal as the sulfhydryl group of **2** in complex with ACE–Zn.[29] It therefore seems likely that mercaptocarboxylate inhibitors of zinc hydrolases can interact with the zinc ion(s) of their target enzymes *via* either their carboxylate or their thiolate groups. It cannot be excluded that the mode of binding of **2** to CphA is influenced by the experimental conditions, *i.e.* higher pH values may favor sulfhydryl group ionisation, leading to better interaction with the metal ion.

To investigate the importance of the thiol group of **2** for inhibition of CphA and to test the results obtained by crystallographic studies, non-thiol derivatives of **2** were then synthesised (Fig. 3, and Scheme 1 compounds **9** and **10**) and tested for inhibition of CphA and IMP-1. Similarly, non-thiol derivatives of **8b** were also synthesised (Fig. 3 and Scheme 1 compounds **11** and **12**) and screened under the same conditions.

Compound **9** retained a significant level of inhibition of the CphA MBL ($K_i = 189 \pm 12$ μM), suggesting that the thiol group of **2** is not essential for the inhibition of CphA, in support of the crystallographic and modelling studies, indicating the thiol of **2** does not chelate to the zinc. In contrast, **9** was inactive (at 100 μM) against IMP-1, demonstrating that the replacement of the thiol group of **2** is detrimental to the inhibition of IMP-1, consistent with the apparently general mechanism of inhibition of the sub-classes B1 and B3 involving a thiol–zinc chelation. No inhibition was observed when **11** and **12** (at 100 μM) were tested against CphA and IMP-1, possibly reflecting the necessity of the thiolate group for potent inhibition of both monozinc and dizinc MBLs.

Conclusions

This work has demonstrated that it should be possible to develop individual compounds that are potent inhibitors of all three MBL sub-classes. An important structural point that has arisen is that the same compound may bind in different modes to different MBL sub-classes whilst still retaining inhibition activity. Specifically, crystallographic analyses revealed that whilst mercaptocarboxylate was observed to bind to the zinc ion *via* its thiolate group in the cases of the B1 and B3 sub-classes, for the B2 sub-class this binding mode was not observed. Instead, for the B2 CphA enzyme the thiolate group of **2** was observed to bind to the alcohol side chains of Thr119 and Thr157. In some cases, whether or not the thiol inhibitors preferentially bind with one or two zinc ions can be important to the potency of inhibitor observed. Thus, compounds that interact preferentially with monozinc CphA–Zn appear to be more potent than those that induce binding of a second zinc to give CphA–Zn_2 complexes (*e.g.* thiomandelate). The useful role of non-denaturing ESI-MS in rapidly providing data on metal binding stoichiometry, data that is often not easily obtained for metallo-proteins, is highlighted in this aspect of the work.

Overall, although the work reveals further complexities in the way that (thiol) inhibitors bind to different MBL sub-classes, it also suggests that utilisation of different binding modes for the same inhibitor binding to different MBL sub-classes may be a productive route to achieving potent broad-spectrum inhibition.

Experimental

Crystallography

Crystallizations of the wildtype CphA and L1 were performed as described.[5,16] The CphA–Zn–**2** and L1–Zn–**5a** complexes were obtained by incubation (24 hours) of protein crystals in a drop of reservoir in which an excess of **2** or **5a** was added. Before data collection, crystals were transferred to a cryoprotectant solution (reservoir solution containing 20% (v/v) glycerol), then mounted rapidly in loops and flash-cooled. X-Ray data for the CphA–**2** and L1–**5a** complexes were collected at the beamline BM30A of the European Synchrotron Radiation Facility (Grenoble, France) and in-house using a Nonius FR591 rotating anode X-ray generator coupled to a Mar Research Imagine Plate detector,

respectively. Data were processed using the CCP4 programs (Table S1†).[30] Initial phases for the CphA–Zn–**2** and L1–Zn–**5a** complex structures were generated by molecular replacement using the structure of the wildtype CphA and L1, respectively, as starting models (PDB accession code 1X8G and 1SML). Refinement was carried out using Coot[31] and REFMAC (CCP4). The calculation of the first ($F_o - F_c$) electron density map clearly showed the presence of the inhibitor molecules in the active site. Inhibitors were modelled in the map after most of the protein main chain and side chain atoms and most of water molecules were built and refined. Conformational torsion-angle restraints and charges assignments for the **2** and **5a** were obtained using CCP4i Libcheck. Data collection and refinement statistics are shown in Table S1†. Coordinates and structure factors have been deposited with the Protein Data Bank[32] with accession codes 2QDS and 2QDT.

NMR

Singly labelled (^{15}N) BcII protein used in all the NMR experiments was expressed and purified as described previously.[6] Sequence-specific resonance assignments for the BcII enzyme were obtained by using triple resonance experiments and will be published elsewhere. All NMR experiments were carried out in 20 mM MES, 100 mM NaCl, 0.2 mM $ZnCl_2$, pH 6.4 at 298 K. Samples of the inhibitor–enzyme complexes were prepared by addition of microlitre volumes of inhibitor solutions (100–200 mM in MES buffer). 1D ^{1}H and 2D ^{1}H–^{15}N heteronuclear single quantum coherence (HSQC) spectra were used to establish when the complex was fully formed. The NMR spectra were obtained by using Bruker Avance DRX or DMX 600 MHz instruments. 1D ^{1}H spectra were obtained by using a water flip-back pulse combined with Watergate.[33,34] Backbone NH resonances were observed by ^{1}H–^{15}N HSQC with States TPPI and Watergate. The imidazole ^{15}N(C)H resonances were observed by ^{1}H–^{15}N HSQC (heteronuclear single quantum coherence) as previously described.[6] In the absence of resonance assignments for the inhibitor complexes, residues affected by inhibitor binding were identified by using minimum chemical shift approach. Here, the chemical shift difference between an amide cross-peak in the ^{1}H–^{15}N HSQC spectrum of the free protein (whose assignment is known) and the position of the nearest cross-peak in the corresponding spectrum of the enzyme–inhibitor complex is calculated. The ^{1}H and ^{15}N chemical shift differences, ΔH and ΔN, between each pair of cross-peaks provide the minimum chemical shift index based on the following formula:[35]

$$\sqrt{\left(\frac{\Delta H}{0.03}\right)^2 + \left(\frac{\Delta N}{0.3}\right)^2}$$

Whereas the true values of the chemical shift changes may be underestimated, the pattern of interactions observed by this approach has been found in a number of systems to be similar to the pattern seen when assignments are available for both free enzyme and the complex.[26,36]

Kinetic analyses

Solution of **5a** and **5b** were prepared as 10 mM DMSO solutions before dilution with 20 mM HEPES buffer pH 7.0 containing 20 μg mL^{-1} BSA (and 100 μM $ZnCl_2$ where indicated). Tests verified that the low concentrations of DMSO present had no inhibition effects; the rate remained the same upon addition of 1% DMSO. The inhibitors **3**, **4**, **8a–c** were prepared as 100 μM stock solutions directly into the buffer used. For these inhibitors the buffer was 20 mM PIPES buffer pH 6.0 containing 20 μg mL^{-1} BSA (and 100 μM $ZnCl_2$ where indicated). BcII, IMP-1, CphA, L1 and FEZ-1 enzymes were used at fixed concentrations between 0.03 and 0.7 nM. The enzyme and inhibitor were pre-incubated, when found to be necessary (see optimisation below), at room temperature before the substrate was added. Substrate concentrations were varied between 20 and 200 μM at a minimum of 2 inhibitor concentrations and in its absence. Hydrolysis of imipenem and nitrocefin was monitored by following the variation in absorbance at 300 nm or 482 nm respectively, using a Uvikon 860 spectrophotometer connected to a computer *via* a RS232 serial interface. Cells of 2 mm or 10 mm path length were used depending on substrate concentration. The experiments were performed at 30 °C and initial rate conditions were used to study the inhibition with imipenem or nitrocefin using the Hanes linearisation of the Henri–Michaelis equation and the KaleidaGraph 3.5 programme. Since the FEZ-1 MBL did not show competitive inhibition with these inhibitors, the IC_{50} was determined at a substrate concentration of 200 μM nitrocefin.

To optimise preincubation times, an appropriate amount of enzyme was incubated with 100 μM inhibitor in a total volume of 5 mL in 10 mM HEPES buffer pH 7.0 (containing 100 μM $ZnCl_2$ with all enzymes except for CphA) at 30 °C. Samples of 490 μL were removed at various time intervals, 10 μL of 5 mM imipenem or nitrocefin was added and the activity measured at 30 °C.

Docking experiments

The program GOLD[37] (version 3.0) was used for docking analyzes. In GOLD, metal ions are considered to bind to hydrogen bond acceptors in the ligand. Coordination points are added at points around the metal, where coordination sites are missing. Tetrahedral and trigonal bipyramidal geometries were used for zinc metals in dizinc and monozinc MBLs respectively. These coordination points can then bind to acceptor atoms in the ligand. The ligands were prepared using MarvinSketch.[38] The proteins were prepared for docking using WHAT IF.[39] This online program generates proteins with the correct input for docking programs such as GOLD. All water molecules and ligands were removed from the proteins. For the dizinc MBLs the binding site of the ligands was defined as a 20 Å sphere centered at the zinc ion that is coordinated by the triad of zinc-binding histidine residues and default settings were applied. For CphA, the binding site was defined as a 20 Å sphere centered at the single zinc ion.

ESI-MS under mild ionisation conditions

Samples were desalted using a Microcon YM-10 (cut-off = 10 000 Da) centrifugal filters (Millipore, Bedford MA, USA) in 15 mM NH_4Ac buffer (pH 7.5). Seven dilution/concentration steps were performed at 4 °C and 14 000 *g*. The stock enzyme solution was diluted in NH_4OAc buffer to a final concentration of 100 μM. Prior to each experiment, individual thiols were freshly dissolved in DMSO at a final concentration of 100 mM. Each thiol was then diluted to 100 μM in 15 mM ammonium acetate buffer pH 7.5.

Samples were prepared by mixing the thiols and enzyme to a final concentration of 15 μM. An aliquot of this mixture was placed in a 96-well plate and analysed. ESI-MS analyses used a Q-TOF mass spectrometer (Q-TOFmicro Micromass, Altrincham, UK) interfaced with a NanoMate™ chip-based nano-ESI source (Advion Biosciences, Ithaca, NY, USA). Samples were infused to the Q-TOF through the ESI chip (estimated flow rate *ca.* 100 nL min^{-1}). Typically a spraying voltage of 1.70 ± 0.1 kV depending on the "sprayability" of the sample and a sample pressure of 0.25 psi were applied. The instrument was equipped with a standard Z-spray source block. Clusters of $Cs_{(n+1)}I_n$ (1 mg mL^{-1} CsI in 100% methanol) were used for calibration. Calibration and sample acquisitions were performed in the positive ion mode in the range of *m*/*z* 500–5000. Operating conditions for the mass spectrometer were: sample cone voltage 50 V, source temperature 40 °C. Acquisition and scan time were 30 s and 1 s, respectively. The pressure at the interface between the atmospheric source and the high vacuum region was fixed at 6.6 mbar (measured with the roughing pump Pirani gauge) by throttling the pumping line using an Edwards Speedivalve to provide collisional cooling.

Synthesis

General. All solvents used were either anhydrous solvents purchased from Aldrich (Sigma-Aldrich Chemical Co., Dorset, UK) or dried by passing over an alumina column under nitrogen pressure. Reagents were used as obtained from commercial sources unless otherwise stated. Measurement of pH was carried out using Prolabo Rota™ pH 1–10 paper. Flash chromatography was performed using silica gel (0.125–0.25 mm, 60–120 mesh) as the stationary phase. Thin layer chromatography (TLC) was performed on aluminium plates pre-coated with silica gel (Merck silica gel 60 F_{254}), which were visualized by the quenching of UV fluorescence (using an irradiation wavelength $\lambda = 254$ nm), and/or by staining with iodine or 10% ammonium molybdate in 2 M sulfuric acid, followed by heating. Melting points were obtained using a Büchi 510 Cambridge Instruments Gallen III hot stage melting point apparatus. Infrared (IR) spectra were recorded as thin films between NaCl plates or as KBr discs on a Tensor 27 FT-IR Brüker spectrometer. Only selected absorbances are reported. Proton magnetic resonance spectra (^{1}H NMR) were recorded on a Bruker DPX 250 (250 MHz), Bruker DQX 400 (400 MHz), or Bruker AMX500 (500 MHz) spectrometers at ambient temperature. ^{1}H NMR spectral assignments are supported by ^{1}H–^{1}H COSY experiments where necessary. Coupling constant values (*J*) are reported to the nearest 0.5 Hz. Carbon magnetic resonance spectra (^{13}C NMR) were recorded on a Bruker DPX 250 (62.9 MHz), Bruker DQX 400 (100.6 MHz) or Bruker AMX500 (125.8 MHz) spectrometers at ambient temperature. ^{13}C NMR assignments were made using DEPT-135 along with HMQC, and HMBC correlation experiments. High-resolution mass spectra were recorded on a VG Autospec spectrometer by chemical ionization or on a Micromass LCT electrospray ionization mass spectrometer operating at a resolution of 5000 full width half height. High performance liquid chromatography (HPLC) used a Waters 996 photodiode array detector, a Waters 600E system controller and a Waters 717 plus autosampler, with a Phenomenex Synergy 4 μ MAX RP80A (250 × 4.60 mm) column for analytical HPLC and a Phenomenex Luna 5 μ C_{18} (250 × 4.60 mm) column for preparative HPLC.

Methyl 3,5-bis(bromomethyl)benzoate (14). Prepared as previously described.[22] M.p. 96–97 °C (lit.[22] 100–101 °C); ^{1}H NMR (400 MHz, $CDCl_3$): $\delta = 8.01$ (d, 2H, $J = 1.5$ Hz, 2 × ArCH), 7.63 (s, 1H, ArCH), 4.51 (s, 4H, 2 × CH_2), 3.94 ppm (s, 3H, CH_3); ^{13}C NMR (100.6 MHz, $CDCl_3$): $\delta = 165.9$ (C=O), 138.9 (2 × ArC), 133.9 (ArCH), 131.4 (ArC), 130.0 (2 × ArCH), 52.4 (OCH_3), 31.9 (2 × CH_2) ppm; HRMS (CI$^+$): $[M + NH_4]^+$ calcd. for $C_{10}H_{14}NO_2{}^{79}Br^{81}Br$, 339.9371; found, 339.9377.

Methyl 3,5-bis[(acetylsulfanyl)methyl]benzoate (15). Prepared as previously described.[40] ^{1}H NMR (400 MHz, $CDCl_3$): $\delta = 7.84$ (d, 2H, $J = 1.5$ Hz, 2 × ArCH), 7.41 (s, 1H, ArCH), 4.12 (s, 4H, 2 × CH_2), 3.91 (s, 3H, CH_3), 2.36 ppm (s, 6H, 2 × CH_3); ^{13}C NMR (100.6 MHz, $CDCl_3$): $\delta = 194.7$ (2 × CH_3C=O), 166.5 (ArC=O), 138.6 (2 × ArC), 133.7 (ArCH), 130.9 (ArC), 128.9 (2 × ArCH), 52.3 (OCH_3), 32.9 (2 × CH_2), 30.4 ppm (2 × CH_3CO); HRMS (ES$^+$): $[M + NH_4]^+$ calcd. for $C_{14}H_{20}NO_4S_2$, 330.0834; found, 330.0833.

3,5-Bis(sulfanylmethyl)benzoic acid (3). Prepared as previously described.[22] M.p. 121–123 °C (lit.[22] 133 °C); ^{1}H NMR (400 MHz, DMSO-d_6): $\delta = 7.90$ (d, 2H, $J = 1.5$ Hz, 2 × ArCH), 7.59 (s, 1H, ArCH), 3.80 (s, 4H, 2 × CH_2); ^{13}C NMR (125.8 MHz, DMSO-d_6): $\delta = 167.1$ (C=O), 142.4 (2 × ArC), 132.5 (ArCH), 131.1 (ArC), 127.5 (2 × ArCH), 27.3 ppm (2 × CH_2); MS (ES$^-$): *m*/*z* (%): 213 (100) $[M - H]^-$.

(*S*)-(2-Oxo-2-phenylethyl) ethanethioate (17). Prepared as previously described.[40] ^{1}H NMR (400 MHz, $CDCl_3$): $\delta = 8.01$–7.98 (m, 2H, 2 × ArCH), 7.63–7.58 (m, 1H, ArCH), 7.51–7.47 (m, 2H, 2 × ArCH), 4.41 (s, 2H, CH_2), 2.41 ppm (s, 3H, CH_3); ^{13}C NMR (100.6 MHz, $CDCl_3$): $\delta = 194.2$ (C=O), 193.2 (C=O), 135.5 (ArC), 133.8 (ArC), 128.8 (2 × ArCH), 128.5 (2 × ArCH), 36.7 (CH_2), 30.3 ppm (CH_3); MS (ES$^+$): *m*/*z* (%): 195 (100) $[M + H]^+$.

1-Phenyl-2-sulfanylethanone (4). An aqueous solution of 1 N NaOH (8.25 mL, 8.25 mmol, 4 eq) was added to **17** (400 mg, 2.06 mmol, 1 eq) under a nitrogen atmosphere. The resulting mixture was stirred at 22 °C for 6 h. The reaction mixture was acidified with HCl (10 N) and extracted with EtOAc (2 × 20 mL). The combined organic extracts were washed with brine (2 × 20 mL), dried over $MgSO_4$ and the solvent removed under reduced pressure. Purification by flash chromatography using a mixture of CH_2Cl_2–petroleum ether (40–60)–AcOH (20 : 80 : 1) as eluent afforded 216 mg (69%) of **4** as a colourless oil. ^{1}H NMR (400 MHz, $CDCl_3$): $\delta = 7.98$–7.96 (m, 2H, 2 × ArCH), 7.63–7.59 (m, 1H, ArCH), 7.52–7.48 (m, 2H, 2 × ArCH), 3.98 (d, 2H, $J = 7.5$ Hz, CH_2), 2.15 ppm (t, 1H, $J = 7.5$ Hz, SH); ^{13}C NMR (100.6 MHz, $CDCl_3$): $\delta = 194.8$ (C=O), 135.0 (ArC), 133.7 (ArC), 128.9 (2 × ArCH), 128.5 (2 × ArCH), 31.2 ppm (CH_2); HRMS (CI$^+$): $[M + H]^+$ calcd. for C_8H_9OS, 153.0374; found, 153.0370.

(*R*)-Methyl 2-(3-bromopropanamido)-3-phenylpropanoate (18). Prepared as previously described.[41] IR ν_{max} (film): 3055, 2953, 1739 (C=O), 1681 (C=O), 1266, 739 cm^{-1}; ^{1}H NMR (400 MHz, $CDCl_3$): $\delta = 6.19$ (brs, 1H, NH), 4.64 (p, 1H, $J = 7$ Hz, CHα), 3.77 (s, 3H, OCH_3), 3.66–3.63 (m, 2H, CH_2), 2.81–2.78 (m, 2H, CH_2), 1.44 ppm (d, 3H, $J = 7.0$ Hz, CH_3); ^{13}C NMR (100.6 MHz, $CDCl_3$): $\delta = 173.8$ (C=O), 169.5 (C=O), 53.0 (OCH_3), 48.6 (CHα),

39.9 (CH_2), 27.4 (CH_2), 19.0 ppm (CH_3); HRMS (ES^+): $[M + H]^+$ calcd. for $C_7H_{13}NO_3Br$, 238.0079; found, 238.0081.

(*R*)-Methyl 2-(3-(acetylthio)propanamido)propanoate (23). Prepared as previously described.[40] IR ν_{max} (film): 3055, 2987, 1742 (C=O), 1686 (C=O), 1266, 739 cm^{-1}; ^1H NMR (400 MHz, $CDCl_3$): $\delta = 6.20$ (brs, 1H, NH), 4.59 (p, 1H, $J = 7.5$ Hz, CHα), 3.74 (s, 3H, OCH_3), 3.13 (t, 2H, $J = 7$ Hz, CH_2), 2.52 (t, 2H, $J = 7$ Hz, CH_2), 2.32 (s, 3H, CH_3COS), 1.40 ppm (d, 3H, $J = 7.5$ Hz, $CH_3\beta$); ^{13}C NMR (100.6 MHz, $CDCl_3$): $\delta = 196.0$ (C=O), 173.4 (C=O), 170.1 (C=O), 52.5 (OCH_3), 48.1 (CHα), 36.0 (CH_2), 30.6 (CH_3COS), 24.7 (CH_2), 18.4 ppm ($CH_3\beta$); HRMS (ES^+): $[M + H]^+$ calcd. for $C_9H_{16}NO_4S$, 234.0800; found, 234.0802.

(*R*)-2-(3-Mercaptopropanamido)propanoic acid (5a). Prepared as previously described.[23] M.p. 78–79 °C (lit.[23] 79–81 °C); ^1H NMR (250 MHz, CD_3OD): $\delta = 4.41$ (q, 1H, $J = 7.5$ Hz, CHα), 2.82–2.78 (m, 2H, CH_2), 2.57–2.54 (m, 2H, CH_2), 1.42 ppm (d, 3H, $J = 7.5$ Hz); MS (ES^-): *m/z* (%): 176 (100) $[M - H]^-$; $[\alpha]_D^{25} = +39$ (MeOH, $c = 0.5$).

(*S*)-2-(3-Mercaptopropanamido)propanoic acid (5b). **5b** and its reaction intermediates (**19** and **24**) were obtained following the same procedure that leading to **5a**. All analytical data for **5b** were identical to that of **5a** with the exception of the optical rotation (−39.5 (MeOH, $c = 0.5$)).

(*R*)-Methyl 2-(3-bromopropanamido)-2-phenylacetate (20). Prepared as previously described.[41] M.p. 61–62 °C; IR ν_{max} (film): 3019, 1741 (C=O), 1679 (C=O), 1216, 756 cm^{-1}; ^1H NMR (400 MHz, $CDCl_3$): $\delta = 7.38$–7.33 (m, 5H, 5 × ArCH), 6.73 (d, 1H, $J = 7$ Hz, NH), 5.60 (d, 1H, $J = 7$ Hz, CHα), 3.74 (s, 3H, OCH_3), 3.61 (t, 2H, $J = 7$ Hz, CH_2), 2.90–2.76 ppm (m, 2H, CH_2); ^{13}C NMR (100.6 MHz, $CDCl_3$): $\delta = 171.2$ (C=O), 169.0 (C=O), 136.2 (ArC), 129.0 (2 × ArCH), 128.6 (ArCH), 127.3 (2 × ArCH), 56.5 (CHα), 52.9 (OCH_3), 39.3 (CH_2), 26.8 ppm (CH_2); HRMS (ES^+): $[M + H]^+$ calcd. for $C_{12}H_{15}NO_3Br$, 300.0235; found, 300.0226; $[\alpha]_D^{25} = -145$ ($CHCl_3$, $c = 0.45$).

(*R*)-Methyl 2-(3-(acetylthio)propanamido)-2-phenylacetate (25). Prepared as previously described.[40] M.p. 48–50 °C; IR ν_{max} (film): 1741 (C=O), 1684 (C=O), 909, 734 cm^{-1}; ^1H NMR (400 MHz, $CDCl_3$): $\delta = 7.34$ (m, 5H, 5 × ArCH), 6.69 (d, 1H, $J = 7$ Hz, NH), 5.57 (d, 1H, $J = 7$ Hz), 3.72 (s, 3H, OCH_3), 3.11 (t, 2H, $J = 7$ Hz, CH_2), 2.56 (m, 2H, CH_2), 2.30 ppm (s, 3H, CH_3COS); ^{13}C NMR (100.6 MHz, $CDCl_3$): $\delta = 196.0$ (C=O), 171.2 (C=O), 170.1 (C=O), 136.3 (ArC), 129.0 (2 × ArCH), 128.6 (ArCH), 127.3 (2 × ArCH), 56.4 (CHα), 52.8 (OCH_3), 35.9 (CH_2), 30.5 (CH_3COS), 24.6 ppm (CH_2); HRMS (ES^+): $[M + H]^+$ calcd. for $C_{14}H_{18}NO_4S$, 296.0957; found, 296.0959; $[\alpha]_D^{25} = -124$ ($CHCl_3$, $c = 0.10$).

(*RS*)-2-(3-Mercaptopropanamido)-2-phenylacetic acid (8a). Prepared as previously described.[23] M.p. 105–108 °C (lit.[42] 102–106 °C); ^1H NMR (250 MHz, CD_3OD): $\delta = 7.49$–7.34 (m, 5H, 5 × ArCH), 5.48 (s, 1H, CHα), 2.78–2.69 (m, 2H, CH_2), 2.67–2.56 ppm (m, 2H, CH_2); MS (ES^-): *m/z* (%): 238 (30) $[M - H]^-$.

(*R*)-Methyl 2-(3-bromopropanamido)-3-phenylpropanoate (21). Prepared as previously described.[41] M.p. 54–55 °C; IR ν_{max} (film): 3056, 2954, 1743 (C=O), 1665 (C=O), 1266, 738 cm^{-1}; ^1H NMR (400 MHz, $CDCl_3$): $\delta = 7.30$–7.24 (m, 3H, 3 × ArCH), 7.13–7.11 (m, 2H, 2 × ArCH), 6.24 (d, 1H, $J = 7$ Hz, NH), 4.92 (m, 1H, CHα), 3.73 (s, 3H, OCH_3), 3.59 (m, 2H, CH_2), 3.16 (AA'B, dd, 1H, $J = 14$ Hz, $J = 5.5$ Hz, $CH_2\beta$), 3.09 (AA'B, dd, 1H, $J = 14$ Hz, $J = 5.5$ Hz, $CH_2\beta$), 2.76 ppm (m, 2H, CH_2); ^{13}C NMR (100.6 MHz, $CDCl_3$): $\delta = 171.9$ (C=O), 169.2 (C=O), 135.7 (ArC), 129.3 (2 × ArCH), 128.6 (2 × ArCH), 127.2 (ArCH), 53.2 (CHα), 52.4 (OCH_3), 39.4 (CH_2), 37.8 ($CH_2\beta$), 27.0 ppm (CH_2); HRMS (ES^+): $[M + H]^+$ calcd. for $C_{13}H_{17}NO_3Br$, 314.0392; found, 314.0390.

(*R*)-Methyl 2-(3-(acetylthio)propanamido)-3-phenylpropanoate (26). Prepared as previously described.[40] IR ν_{max} (film): 3055, 2987, 1743 (C=O), 1686 (C=O), 1266, 737 cm^{-1}; ^1H NMR (400 MHz, $CDCl_3$): $\delta = 7.27$ (m, 3H, 3 × ArCH), 7.10 (m, 2H, 2 × ArCH), 6.02 (d, 1H, $J = 7.5$ Hz, NH), 4.89 (m, 1H, CHα), 3.73 (s, 3H, OCH_3), 3.12 (m, 4H, 2 × CH_2), 2.49 (m, 2H, CH_2), 2.32 ppm (s, 3H, CH_3COS); ^{13}C NMR (100.6 MHz, $CDCl_3$): $\delta = 196.0$ (C=O), 171.9 (C=O), 170.2 (C=O), 135.7 (ArC), 129.3 (2 × ArCH), 128.6 (2 × ArCH), 127.2 (ArCH), 53.1 (CHα), 52.4 (OCH_3), 37.8 (CH_2), 36.0 (CH_2), 30.6 (CH_3COS), 24.7 ppm (CH_2); HRMS (ES^+): $[M + H]^+$ calcd. for $C_{15}H_{20}NO_4S$, 310.1113; found, 310.1104.

(*R*)-2-(3-Mercaptopropanamido)-3-phenylpropanoic acid (8b). Prepared as previously described.[23] M.p. 102–104 °C (lit.[23] 106–107 °C); ^1H NMR (250 MHz, CD_3OD): $\delta = 7.30$–7.25 (m, 5H, 5 × ArCH), 4.75–4.69 (m, 1H, CHα), 3.29–3.20 (m, 1H, $CH_2\beta$), 2.97 (dd, 1H, $J = 9.5$ Hz, $J = 14$ Hz, $CH_2\beta$), 2.64 (m, 2H, CH_2), 2.46 (m, 2H, CH_2); MS (ES^-): *m/z* (%): 253(100) $[M - H]^-$; $[\alpha]_D^{25} = -10.0$ (MeOH, $c = 0.5$).

(*R*)-Methyl 2-(3-bromopropanamido)-4-methylpentanoate (22). Prepared as previously described.[41] IR ν_{max} (film): 3055, 2960, 1742 (C=O), 1677 (C=O), 1266, 740 cm^{-1}; ^1H NMR (400 MHz, $CDCl_3$): $\delta = 6.10$ (d, 1H, $J = 7.5$ Hz, NH), 4.70–4.66 (m, 1H, CHα), 3.74 (s, 3H, OCH_3), 3.64–3.62 (m, 2H, CH_2), 2.83–2.81 (m, 2H, CH_2), 1.68–1.66 (m, 2H, CH_2), 1.57–1.56 (m, 1H, CH), 0.95–0.94 ppm (m, 6H, 2 × CH_3); ^{13}C NMR (100.6 MHz, $CDCl_3$): $\delta = 173.4$ (C=O), 169.4 (C=O), 52.4 (OCH_3), 50.8 (CHα), 41.7 (CH_2), 39.5 (CH_2), 27.1 (CH_2), 24.8 (CH), 22.8 (CH_3), 21.9 ppm (CH_3); HRMS (ES^+): $[M + H]^+$ calcd. for $C_{10}H_{19}NO_3Br$, 280.0548; found, 280.0540.

(*R*)-Methyl 2-(3-(acetylthio)propanamido)-4-methylpentanoate (27). Prepared as previously described.[40] IR ν_{max} (film): 3055, 2960, 1742 (C=O), 1685 (C=O), 1266, 739 cm^{-1}; ^1H NMR (400 MHz, $CDCl_3$): $\delta = 6.02$ (d, 1H, $J = 8$ Hz, NH), 4.66–4.61 (m, 1H, CHα), 3.73 (s, 3H, OCH_3), 3.13 (t, 2H, $J = 7$ Hz, CH_2), 2.53 (t, 2H, $J = 7$ Hz, CH_2), 2.32 (s, 3H, CH_3COS), 1.65–1.60 (m, 2H, CH_2), 1.54–1.50 (m, 1H, CH), 0.94–0.93 ppm (m, 6H, 2 × CH_3); ^{13}C NMR (100.6 MHz, $CDCl_3$): $\delta = 196.1$ (C=O), 173.5 (C=O), 170.4 (C=O), 52.3 (OCH_3), 50.7 (CHα), 41.7 (CH_2), 36.1 (CH_2), 30.6 (CH_3COS), 24.9 (CH), 24.8 (CH_2), 22.8 (CH_3), 22.0 ppm (CH_3); HRMS (ES^+): $[M + H]^+$ calcd. for $C_{12}H_{22}NO_4S$, 276.1270; found, 276.1261.

(*R*)-2-(3-Mercaptopropanamido)-4-methylpentanoic acid (8c). Prepared as previously described.[23] ^1H NMR (400 MHz, CD_3OD): $\delta = 4.50$–4.44 (m, 1H, CHα), 2.82–2.74 (m, 2H, CH_2), 2.59–2.55 (m, 2H, CH_2), 1.79–1.62 (m, 3H, CH + CH_2), 1.00–0.94 ppm (m, 6H, 2 × CH_3); MS (ES^-): *m/z* (%): 218 (100) $[M - H]^-$; $[\alpha]_D^{25} = +32.0$ (MeOH, $c = 0.5$).

(*R*)-Methyl 2-(3-hydroxypropanamido)-3-phenylpropanoate (28). To an ice-cooled suspension of D-phenylalanine methyl ester hydrochloride (1.00 g, 4.64 mmol) in absolute EtOH (10 mL) was added β-propiolactone (0.29 mL, 4.64 mmol) and sodium acetate (380 mg, 4.64 mmol). The resulting mixture was stirred at 22 °C for 15 h. The reaction mixture was partitioned between EtOAc (100 mL) and H_2O (100 mL) and the aqueous phase was extracted with EtOAc (2 × 100 mL). The combined organic extracts were washed with brine (2 × 100 mL), dried over $MgSO_4$ and the solvent removed under reduced pressure. Purification by flash chromatography using a gradient of EtOAc–MeOH (from 99 : 1 to 90 : 10) as eluent afforded 230 mg (21%) of **28** as a colourless oil. ^{1}H NMR (400 MHz, $CDCl_3$): δ = 7.32–7.23 (m, 3H, 3 × PhCH), 7.13–7.11 (m, 2H, 2 × PhCH), 6.34 (brs, 1H, J = 7.5 Hz, NH), 4.93–4.88 (m, 1H, CHα), 3.83 (t, 2H, J = 5.5 Hz, CH_2OH), 3.74 (s, 3H, OCH_3), 3.18 (dd, 1H, J = 5.5 Hz, J = 14.0 Hz, CHβ), 3.08 (dd, 1H, J = 6.5 Hz, J = 14.0 Hz, CHβ), 2.44–2.41 ppm (m, 2H, CH_2C=O); ^{13}C NMR (100.6 MHz, $CDCl_3$): δ = 172.1 (C=O), 170.7 (C=O), 135.7 (PhC), 129.2 (2 × PhCH), 128.6 (2 × PhCH), 127.2 (PhCH), 58.8 (CH_2O), 53.1 (Cα), 52.5 (OCH_3), 38.1 (CH_2C=O), 37.8 ppm (Cβ); HRMS (ES$^-$): [M − H]$^-$ calcd. for $C_{13}H_{16}NO_4$, 250.1074; found, 250.1079.

(*R*)-2-(3-Hydroxypropanamido)-3-phenylpropanoic acid (11). An aqueous solution of 1 N NaOH (2.40 mL, 2.40 mmol) was added to **28** (200 mg, 0.80 mmol). The resulting mixture was stirred at 22 °C for 15 h. The reaction mixture was acidified with HCl (10 N) and extracted with EtOAc (5 × 10 mL). The combined organic extracts were washed with brine (50 mL), dried over $MgSO_4$ and the solvent removed under reduced pressure. Purification by flash chromatography using a mixture of EtOAc–MeOH–AcOH (95 : 5 : 1) as eluent afforded 100 mg (53%) of **11** as a colourless oil. ^{1}H NMR (400 MHz, DMSO-d_6): δ = 8.14 (d, 2H, J = 8.5 Hz, NH), 7.29–7.19 (m, 5H, 5 × PhCH), 4.45–4.41 (m, 1H, CHα), 3.56–3.50 (m, 2H, CH_2OH), 3.04 (dd, 1H, J = 5.0 Hz, J = 14.0 Hz, CHβ), 2.86 (dd, 1H, J = 9.0 Hz, J = 14.0 Hz, CHβ), 2.24 ppm (t, 2H, J = 7.0 Hz, CH_2C=O); ^{13}C NMR (100.6 MHz, DMSO-d_6): δ = 173.5 (C=O), 171.1 (C=O), 138.1 (PhC), 129.6 (2 × PhCH), 128.6 (2 × PhCH), 126.9 (PhCH), 58.0 (CH_2O), 53.8 (Cα), 39.3 (CH_2C=O), 37.3 ppm (CHβ); HRMS (ES$^-$): [M − H]$^-$ calcd. for $C_{12}H_{14}NO_4$, 236.0917; found, 236.0918.

(*R*)-2-Acetamido-3-phenylpropanoic acid (12). Prepared as previously described.[24] ^{1}H NMR (400 MHz, $CDCl_3$): δ = 8.20 (d, 1H, J = 8.0 Hz, NH), 7.30–7.18 (m, 5H, 5 × PhCH), 4.43–4.37 (m, 1H, CHα), 3.04 (dd, 1H, J = 5.0 Hz, J = 14.0 Hz, CHβ), 2.83 (dd, 1H, J = 9.5 Hz, J = 14.0 Hz, CHβ), 1.78 ppm (s, 3H, CH_3); ^{13}C NMR (100.6 MHz, $CDCl_3$): δ = 174.1 (C=O), 170.1 (C=O), 138.6 (ArC), 129.9 (2 × PhCH), 129.0 (2 × PhCH), 127.3 (PhCH), 54.4 (Cα), 37.6 (Cβ), 23.2 ppm (CH_3).

(*R*)-Methyl 4-(*tert*-butyldiphenylsilyloxy)-2-methylbutanoate (30). To a solution of alcohol **29** (1.0 g, 8.46 mmol) in 2.5 mL of DMF were added imidazole (1.15 g, 16.9 mmol) and TBDPSCl (4.4 mL, 8.46 mmol). The mixture was stirred overnight and poured into 50 mL of 1.2 M HCl. The aqueous phase was extracted with diethyl ether (3 × 50 mL) and the organic layer was washed with water and dried over $MgSO_4$. The solvent was removed under reduced pressure to yield (65%) to the desired product as a colourless oil which was used without further purification. ^{1}H NMR ($CDCl_3$, 200 MHz) δ 1.03 (s, 9H), 1.16 (d, J = 7.0 Hz, 3H), 2.72 (m, 1H), 3.69 (s, 3H), 3.76 (m, 2H), 7.3–7.45 (m, 6H), 7.64–7.69 (m, 4H).

(*R*)-4-(*tert*-Butyldiphenylsilyloxy)-2-methylbutanoic acid (31). A solution of 3 N LiOH (4.7 mL) was added dropwise to a stirred and cooled solution of **30** (1.0 g, 2.81 mmol) in 11 mL of THF at 0 °C. To this was added 11 mL of MeOH and the mixture was stirred for 20 h at room temperature. The solution was acidified with 3 N HCl. It was extracted 5 times with diethyl ether. The organic layer was washed with water and dried over $MgSO_4$. The solvent was removed under reduced pressure to yield the desired product as colourless oil (89%), which was used without further purification. ^{1}H NMR ($CDCl_3$, 200 MHz) δ 1.07 (s, 9H), 1.18 (d, J = 7.0 Hz, 3H), 2.75 (m, 1H), 3.82 (m, 2H), 7.30–7.47 (m, 6H), 7.64–7.73 (m, 4H).

(*R*)-1-((*R*)-4-(*tert*-Butyldiphenylsilyloxy)-2-methylbutanoyl)pyrrolidine-2-carboxylic acid (32). Oxalyl chloride (0.3 mL, 3.44 mmol) was added to a stirred and cooled solution of **31** (0.46 g, 1.34 mmol) in 3.9 mL of dry benzene at 0 °C under an atmosphere of argon. The mixture was stirred for 1h at 0 °C. Then oxalyl chloride (0.18 mL, 2.06 mmol) was again added and the stirring was continued at 0 °C for 2 h. The mixture was concentrated *in vacuo* to give the acid chloride, which was used without further purification. The acid chloride in 10 mL of CH_2Cl_2 was added dropwise to a solution of the corresponding proline (136 mg, 1.18 mmol) and triethylamine (164 µL, 1.18 mmol) in 10 mL of CH_2Cl_2. After stirring at room temperature for 18 h, the mixture was washed twice with water, dried with $MgSO_4$, and evaporated to give the desired product (76%) as colourless oil. ^{1}H NMR ($CDCl_3$, 200 MHz) δ 1.01–1.08 (m, 9H), 1.15–1.26 (m, 3H), 1.75–2.40 (m, 3H), 2.60–3.10 (m, 2H), 3.45–3.95 (m, 3H), 4.50–4.65 (m, 1H), 7.3–7.5 (m, 6H), 7.6–7.8 (m, 4H). Anal. Calcd for $C_{25}H_{33}O_4SiN$ (439.63): C, 68.30; H, 7.57; N, 3.19. Found: C, 67.97; H, 7.49; N, 3.33.

(*R*)-1-((*R*)-4-Hydroxy-2-methylbutanoyl)pyrrolidine-2-carboxylic acid (9). To a solution of **32** (256 mg, 0.58 mmol) in 10 mL of THF was added 0.5 mL of HF·pyridine. The mixture was stirred overnight at room temperature and then evaporated. Water and AcOEt were added and the aqueous phase was freeze-dried to give the crude compounds which was then purified by HPLC (ODS column, λ = 218 nm, NH_4HCO_3 25 mM, pH= 7.5) to yield the desired product (50%) as a white solid. M.p. 250–280 °C (dec.). ^{1}H NMR (D_2O, 400 MHz) δ 0.82–0.83 and 0.89–0.98 (m, 3H), 1.69–1.95 (m, 3H), 2.05–2.19 (m, 1H), 2.27–2.37 and 2.40–2.61 and 2.70–2.87 (m, 1H), 3.30–3.66 (m, 4H), 3.95–4.11 and 4.28–4.34 (m, 1H). ^{13}C NMR ($CDCl_3$, 62.9 MHz) δ 13.0, 13.1, 23.1, 24.7, 29.9, 31.7, 40.6, 41.1, 47.5, 48.2, 63.1, 64.3, 65.0, 172.9, 173.1, 177.1. IR (KBr) 3432, 1616, 1399 cm^{-1}. LRMS APCI$^-$ m/z 200.4 ([M − H]$^-$, 100). $[\alpha]_D^{25}$ = +26.5 (H_2O pH = 7.3, c = 0.52). Anal. Calcd for $C_9H_{15}NO_4$ (201.22): C, 53.72; H, 7.51; N, 6.96. Found: C, 53.64; H, 7.41; N, 7.11.

(*R*)-1-Isobutyrylpyrrolidine-2-carboxylic acid (10). To a solution of D-proline (0.2 g, 1.74 mmol) in CH_2Cl_2 (15 mL) and triethylamine (183 µL, 1.74 mmol) was added dropwise at −10 °C in an atmosphere of argon a solution of isobutyryl chloride (183 µL, 1.74 mmol) in CH_2Cl_2 (15 mL). The mixture was stirred at room temperature for 18 h and then washed twice with water

and dried over $MgSO_4$. The solvent was filtered and evaporated under reduced pressure to give **10** as a white solid (73%). M.p. 112 °C (dec.). ^{1}H NMR (D_2O, 250 MHz) δ 1.19 and 1.22 (2 × d, J = 7.0 Hz, 2 × 3H), 1.93–2.15 and 2.44–2.52 (2 × m, 4H), 2.74 (m, 1H), 3.50–3.73 (m, 2H), 4.63 (m, 1H). ^{13}C NMR (D_2O, 62.9 MHz) δ 18.9, 19.2, 25.1, 28.5, 32.8, 47.7, 58.8, 174.4, 178.4. IR (KBr) 3434, 1723, 1600 cm^{-1}. LRMS APCI$^-$ m/z 184.4 ([M − H]$^-$, 100). Anal. Calcd for $C_9H_{15}NO_3$ (185.22): C, 58.36; H, 8.13; N, 7.56. Found C, 58.21; H, 8.25; N, 7.19.

Acknowledgements

We thank the Biotechnology and Biological Science Research Council and the E.U. (contract no HPRN-CT-2002-00264) for funding and Amura for a CASE award to BMRL. We also thank Carine Bebrone for CphA.

References

1 T. R. Walsh, M. A. Toleman, L. Poirel and P. Nordmann, *Clin. Microbiol. Rev.*, 2005, **18**, 306–325.
2 A. Felici, G. Amicosante, A. Oratore, R. Strom, P. Ledent, B. Joris, L. Fanuel and J. M. Frere, *Biochem. J.*, 1993, **291**, 151–155.
3 B. Segatore, O. Massidda, G. Satta, D. Setacci and G. Amicosante, *Antimicrob. Agents Chemother.*, 1993, **37**, 1324–1328.
4 M. Hernandez Valladares, A. Felici, G. Weber, H. W. Adolph, M. Zeppezauer, G. M. Rossolini, G. Amicosante, J. M. Frere and M. Galleni, *Biochemistry*, 1997, **36**, 11534–11541.
5 G. Garau, C. Bebrone, C. Anne, M. Galleni, J. M. Frere and O. Dideberg, *J. Mol. Biol.*, 2005, **345**, 785–795.
6 C. Damblon, C. Prosperi, L. Y. Lian, I. Barsukov, R. P. Soto, M. Galleni, J. M. Frere and G. C. K. Roberts, *J. Am. Chem. Soc.*, 1999, **121**, 11575–11576.
7 C. Damblon, M. Jensen, A. Ababou, I. Barsukov, C. Papamicael, C. J. Schofield, L. Olsen, R. Bauer and G. C. Roberts, *J. Biol. Chem.*, 2003, **278**, 29240–29251.
8 N. O. Concha, C. A. Janson, P. Rowling, S. Pearson, C. A. Cheever, B. P. Clarke, C. Lewis, M. Galleni, J. M. Frere, D. J. Payne, J. H. Bateson and S. S. Abdel-Meguid, *Biochemistry*, 2000, **39**, 4288–4298.
9 J. H. Toney, G. G. Hammond, P. M. Fitzgerald, N. Sharma, J. M. Balkovec, G. P. Rouen, S. H. Olson, M. L. Hammond, M. L. Greenlee and Y. D. Gao, *J. Biol. Chem.*, 2001, **276**, 31913–31918.
10 C. Mollard, C. Moali, C. Papamicael, C. Damblon, S. Vessilier, G. Amicosante, C. J. Schofield, M. Galleni, J. M. Frere and G. C. Roberts, *J. Biol. Chem.*, 2001, **276**, 45015–45023.
11 U. Heinz, R. Bauer, S. Wommer, W. Meyer-Klaucke, C. Papamichaels, J. Bateson and H. W. Adolph, *J. Biol. Chem.*, 2003, **278**, 20659–20666.
12 J. D. Buynak, H. Chen, L. Vogeti, V. R. Gadhachanda, C. A. Buchanan, T. Palzkill, R. W. Shaw, J. Spencer and T. R. Walsh, *Bioorg. Med. Chem. Lett.*, 2004, **14**, 1299–1304.
13 Q. Sun, A. Law, M. W. Crowder and H. M. Geysen, *Bioorg. Med. Chem. Lett.*, 2006, **16**, 5169–5175.
14 N. Selevsek, A. Tholey, E. Heinzle, B. M. Lienard, N. J. Oldham, C. J. Schofield, U. Heinz, H. W. Adolph and J. M. Frere, *J. Am. Soc. Mass Spectrom.*, 2006, **17**, 1000–1004.
15 A. Carfi, E. Duee, M. Galleni, J. M. Frere and O. Dideberg, *Acta Crystallogr., Sect. D: Biol. Crystallogr.*, 1998, **54**, 313–323.
16 J. H. Ullah, T. R. Walsh, I. A. Taylor, D. C. Emery, C. S. Verma, S. J. Gamblin and J. Spencer, *J. Mol. Biol.*, 1998, **284**, 125–136.
17 I. Garcia-Saez, P. S. Mercuri, C. Papamicael, R. Kahn, J. M. Frere, M. Galleni, G. M. Rossolini and O. Dideberg, *J. Mol. Biol.*, 2003, **325**, 651–660.
18 J. Gao, X. Cheng, R. Chen, G. B. Sigal, J. E. Bruce, B. L. Schwartz, S. A. Hofstadler, G. A. Anderson, R. D. Smith and G. M. Whitesides, *J. Med. Chem.*, 1996, **39**, 1949–1955.
19 J. L. Benesch and C. V. Robinson, *Curr. Opin. Struct. Biol.*, 2006, **16**, 245–251.
20 A. J. Heck and R. H. Van Den Heuvel, *Mass Spectrom. Rev.*, 2004, **23**, 368–389.
21 J. A. Loo, *Mass Spectrom. Rev.*, 1997, **16**, 1–23.
22 H. A. Staab and R. G. H. Kirrstetter, *Liebigs Ann. Chem.*, 1979, **6**, 886–898.
23 M. A. Ondetti and D. W. Cushman, *Ger. Pat.* DE 2717548, 1977.
24 H. K. Chenault, J. Dahmer and G. M. Whitesides, *J. Am. Chem. Soc.*, 1989, **111**, 6354–6364.
25 S. Bounaga, M. Galleni, A. P. Laws and M. I. Page, *Bioorg. Med. Chem.*, 2001, **9**, 503–510.
26 R. A. Williamson, M. D. Carr, T. A. Frenkiel, J. Feeney and R. B. Freedman, *Biochemistry*, 1997, **36**, 13882–13889.
27 I. Garcia-Saez, J. Hopkins, C. Papamicael, N. Franceschini, G. Amicosante, G. M. Rossolini, M. Galleni, J. M. Frere and O. Dideberg, *J. Biol. Chem.*, 2003, **278**, 23868–23873.
28 R. Natesh, S. L. U. Schwager, H. R. Evans, E. D. Sturrock and K. R. Acharya, *Biochemistry*, 2004, **43**, 8718–8724.
29 R. Natesh, S. L. U. Schwager, E. D. Sturrock and K. R. Acharya, *Nature*, 2003, **421**, 551–554.
30 S. Bailey, *Acta Crystallogr., Sect. D: Biol. Crystallogr.*, 1994, **50**, 760–763.
31 P. Emsley and K. Cowtan, *Acta Crystallogr., Sect. D: Biol. Crystallogr.*, 2004, **60**, 2126–2132.
32 H. M. Berman, J. Westbrook, Z. Feng, G. Gilliland, T. N. Bhat, H. Weissig, I. N. Shindyalov and P. E. Bourne, *Nucleic Acids Res.*, 2000, **28**, 235–242.
33 H. Kuboniwa, S. Grzesiek, F. Delaglio and A. Bax, *J. Biomol. NMR*, 1994, **4**, 871–878.
34 M. Piotto, V. Saudek and V. Sklenar, *J. Biomol. NMR*, 1992, **2**, 661–665.
35 L. Y. Lian, I. Barsukov, A. P. Golovanov, D. I. Hawkins, R. Badii, K. H. Sze, N. H. Keep, G. M. Bokoch and G. C. K. Roberts, *Structure*, 2000, **8**, 47–55.
36 F. W. Muskett, T. A. Frenkiel, J. Feeney, R. B. Freedman, M. D. Carr and R. A. Williamson, *J. Biol. Chem.*, 1998, **273**, 21736–21743.
37 G. Jones, P. Willett, R. C. Glen, A. R. Leach and R. Taylor, *J. Mol. Biol.*, 1997, **267**, 727–748.
38 http://www.chemaxon.com/marvin/.
39 http://swift.cmbi.kun.nl/WIWWWI/.
40 G. J. Bodwell, J. N. Bridson, S. L. Chen and R. A. Poirier, *J. Am. Chem. Soc.*, 2001, **123**, 4704–4708.
41 J. Geiwiz, E. Goetschi and P. Hebeisen, *Synthesis*, 2003, 1699–1704.
42 J. L. Stanton, N. Gruenfeld, J. E. Babiarz, M. H. Ackerman, R. C. Friedmann, A. M. Yuan and W. Macchia, *J. Med. Chem.*, 1983, **26**, 1267–1277.

